



# Diffusion Tensor Imaging of the Evolving Response to Mild Traumatic Brain Injury in Rats

Journal of Experimental Neuroscience  
Volume 13: 1–12  
© The Author(s) 2019  
Article reuse guidelines:  
sagepub.com/journals-permissions  
DOI: 10.1177/1179069519858627



Wouter S Hoogenboom<sup>1,2</sup>, Todd G Rubin<sup>1,3</sup> , Kenny Ye<sup>4</sup>,  
Min-Hui Cui<sup>1,5</sup>, Kelsey C Branch<sup>1</sup>, Jinyuan Liu<sup>1</sup>,  
Craig A Branch<sup>1,6,5</sup> and Michael L Lipton<sup>1,3,5,7</sup> 

<sup>1</sup>The Gruss Magnetic Resonance Research Center, Albert Einstein College of Medicine, Montefiore Medical Center, Bronx, NY, USA. <sup>2</sup>Department of Clinical Investigation, Albert Einstein College of Medicine, Montefiore Medical Center, Bronx, NY, USA. <sup>3</sup>Dominick P. Purpura Department of Neuroscience, Albert Einstein College of Medicine, Montefiore Medical Center, Bronx, NY, USA. <sup>4</sup>Department of Epidemiology & Population Health, Albert Einstein College of Medicine, Montefiore Medical Center, Bronx, NY, USA. <sup>5</sup>Department of Radiology, Albert Einstein College of Medicine, Montefiore Medical Center, Bronx, NY, USA. <sup>6</sup>Department of Physiology and Biophysics, Albert Einstein College of Medicine, Montefiore Medical Center, Bronx, NY, USA. <sup>7</sup>Department of Psychiatry and Behavioral Sciences, Albert Einstein College of Medicine, Montefiore Medical Center, Bronx, NY, USA.

**ABSTRACT:** Mild traumatic brain injury (mTBI), also known as concussion, is a serious public health challenge. Although most patients recover, a substantial minority suffers chronic disability. The mechanisms underlying mTBI-related detrimental effects remain poorly understood. Although animal models contribute valuable preclinical information and improve our understanding of the underlying mechanisms following mTBI, only few studies have used diffusion tensor imaging (DTI) to study the evolution of axonal injury following mTBI in rodents. It is known that DTI shows changes after human concussion and the role of delineating imaging findings in animals is therefore to facilitate understanding of related mechanisms. In this work, we used a rodent model of mTBI to investigate longitudinal indices of axonal injury. We present the results of 45 animals that received magnetic resonance imaging (MRI) at multiple time points over a 2-week period following concussive or sham injury yielding 109 serial observations. Overall, the evolution of DTI metrics following concussive or sham injury differed by group. Diffusion tensor imaging changes within the white matter were most noticeable 1 week following injury and returned to baseline values after 2 weeks. More specifically, we observed increased fractional anisotropy in combination with decreased radial diffusivity and mean diffusivity, in the absence of changes in axial diffusivity, within the white matter of the genu corpus callosum at 1 week post-injury. Our study shows that DTI can detect microstructural white matter changes in the absence of gross abnormalities as indicated by visual screening of anatomical MRI and hematoxylin and eosin (H&E)-stained sections in a clinically relevant animal model of mTBI. Whereas additional histopathologic characterization is required to better understand the neurobiological correlates of DTI measures, our findings highlight the evolving nature of the brain's response to injury following concussion.

**KEYWORDS:** Animal model, closed head, concussion, magnetic resonance imaging, modified controlled cortical impact

**RECEIVED:** January 15, 2019. **ACCEPTED:** May 29, 2019.

**TYPE:** Traumatic Brain Injury and Chronic Traumatic Encephalopathy - Original Research

**FUNDING:** The author(s) disclosed receipt of the following financial support for the research, authorship, and/or publication of this article: This research was supported by NIH/National Center for Advancing Translational Sciences (NCATS) Einstein-Montefiore CTSA (Grant No. TL1TR001072), Burroughs Wellcome Foundation Grant (PUP program), NIH/National Institute of Neurological Disorders and Stroke (R01 NS082432), and a grant from the Dana Foundation.

**DECLARATION OF CONFLICTING INTERESTS:** The author(s) declared no potential conflicts of interest with respect to the research, authorship, and/or publication of this article.

**CORRESPONDING AUTHORS:** Michael L Lipton, The Gruss Magnetic Resonance Research Center, Albert Einstein College of Medicine, Montefiore Medical Center, Jack and Pearl Resnick Campus, 1300 Morrispark Avenue, Bronx, NY 10461, USA. Email: michael.lipton@einstein.yu.edu

Craig A Branch, The Gruss Magnetic Resonance Research Center, Albert Einstein College of Medicine, Montefiore Medical Center, Jack and Pearl Resnick Campus, 1300 Morrispark Avenue, Bronx, NY 10461, USA. Email: craig.branch@einstein.yu.edu

## Introduction

Mild traumatic brain injury (mTBI), also known as concussion, is a serious public health issue with an estimated 40 million cases worldwide every year.<sup>1</sup> Although most people who suffer from a concussion make a full recovery within a few weeks, a substantial minority of patients experience chronic dysfunction and disability<sup>2</sup> such as headaches, dizziness, behavioral abnormalities, memory dysfunction, and motor control impairment.<sup>3</sup> The underlying mechanisms contributing to these detrimental effects remain poorly understood and require further research. Although various definitions of mTBI exist based on clinical features,<sup>2</sup> concussion is typically characterized by closed-skull (ie, non-penetrating) injury<sup>4</sup> and the absence of visible findings on routine clinical

computed tomography (CT) and magnetic resonance imaging (MRI), such as skull fracture, hemorrhage, edema, and ischemia.

Diffusion tensor imaging (DTI) has emerged as an MRI method able to detect microstructural damage not visible on standard anatomical images<sup>5</sup> by characterizing the directional coherence of water diffusion *in vivo*.<sup>6</sup> Because diffusion in healthy white matter is highly anisotropic (directional), loss of diffusion anisotropy generally reflects ultrastructural changes in the brain caused by axonal injury, demyelination, and other pathologic processes. Fractional anisotropy (FA) and mean diffusivity (MD) are the most commonly reported DTI-derived metrics believed to reflect overall white matter health, maturation, and organization.<sup>6,7</sup> Axial diffusivity (AD) and radial



Creative Commons Non Commercial CC BY-NC: This article is distributed under the terms of the Creative Commons Attribution-NonCommercial 4.0 License (<http://www.creativecommons.org/licenses/by-nc/4.0/>) which permits non-commercial use, reproduction and distribution of the work without further permission provided the original work is attributed as specified on the SAGE and Open Access pages (<https://us.sagepub.com/en-us/nam/open-access-at-sage>).

diffusivity (RD) are components of FA and MD, which may better inform on underlying injury mechanisms.<sup>8</sup>

The study of human mTBI is complicated by the heterogeneity of underlying pathology due to differences in the characteristics of each injury.<sup>2,9</sup> In addition, pathologic evaluation of tissue injury is not possible in human mTBI. On the other hand, behavioral measures in rodents may not reflect the domains of function experienced by humans. Nonetheless, animal models of mTBI can address some of these limitations because they enable reproducible trauma and the systematic variation of experimental parameters. Moreover, the detection of similar imaging findings in rodents and humans can serve as a translational bridge to link human injury to pathologic mechanisms.

Various animal models have been developed to reproduce the biomechanical, neurological, and pathological aspects observed in human concussion. The methods to produce head injury are generally based on weight drop, fluid percussion, or piston-controlled impact. Detailed descriptions of these methods, as well as their strengths and limitations, have been published elsewhere.<sup>10–12</sup> Briefly, clinically relevant models of experimental concussion should use minimally invasive head impact methods (ie, closed head impact), induce mild injury, and exhibit symptoms in the absence of gross neuropathology.<sup>13</sup>

However, the best characterized and mostly used TBI models to date have employed models of relatively severe TBI in that they induce gross brain pathology or significant axonal death using penetrating head impact methods (eg, controlled cortical impact or lateral fluid percussion).<sup>14</sup> Only few DTI studies have proven to reliably detect TBI and approximate time of injury<sup>15</sup> in various rodent models of axonal injury following single or repetitive head impact.<sup>15–21</sup> Moreover, few studies have assessed the evolution of axonal injury over time following mTBI in rodents. It has been suggested that longitudinal studies are needed to determine how changes in DTI indices are related to recovery in response to concussive injury.<sup>19,22</sup> Such imaging findings can facilitate understanding of injury mechanisms following concussion.

In this report, we present DTI findings of multiple assessments in the first 2 weeks after injury in a rodent model of very mild TBI in which no apparent pathology is visible with conventional MRI or standard histopathology, but significant DTI changes are detected in several white matter areas.

## Materials and Methods

This study followed the National Research Council's "Guide for the care and use of laboratory animals"<sup>23</sup> and was approved by The Institutional Animal Care and Use Committee (IACUC) of Albert Einstein College of Medicine. The experimental design of this study is summarized in Figure 1.

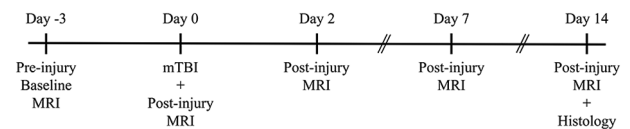


**Figure 1.** Schematic time line of the experimental design. Animals underwent pre-injury baseline MRI at least 3 days before mTBI induction followed by MRI acutely (ie, <4 hours) and 2, 7, and 14 days post-injury. Immediately after the final imaging time point (14 days), animals were sacrificed for histological analysis. MRI indicates magnetic resonance imaging; mTBI, mild traumatic brain injury.

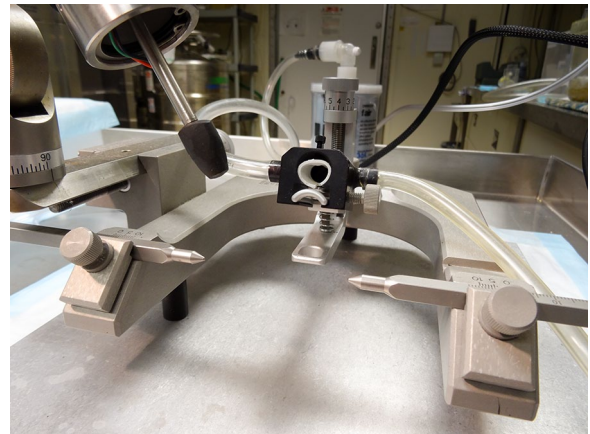


**Figure 2.** Impact device. A modified cortical contusion device (Leica Microsystems Inc, Buffalo Grove, IL) was used to produce a very mild, closed-skull traumatic brain injury. Note the rubber impactor tip.

## Animals

Six- to eight-week-old male Sprague Dawley rats (180 g) were purchased from Charles River Laboratories and housed in standard cages with food and water ad libitum under 12-hour light/dark cycles. A total of 45 animals were used for the study and randomly divided into 2 groups: mTBI injury (n = 35) or sham injury (n = 10).

## Head impact procedure

Rats were anesthetized with isoflurane in room air (3% induction, 1.5%–2% maintenance) and placed in a stereotaxic frame with ear bars for rigid head fixation (David Kopf Inst., Tujunga, CA; Figure 2). The scalp was retracted from the left side of the skull and mild TBI was induced by a single lateral impact (5 mm lateral to midline, 3 mm rostral to bregma; impact velocity = 5 m/s, impact depth = 2 mm, dwell = 100 ms) to the exposed skull using an electromagnetic impactor (Leica Microsystems Inc, Buffalo Grove, IL) modified with a neoprene rubber tip (5 mm diameter, 4 mm thick). Sham-injured rats received the same treatment, including scalp incision and firing of the impactor, but an actual skull impact was not delivered. We discarded 2 animals from the original group due to

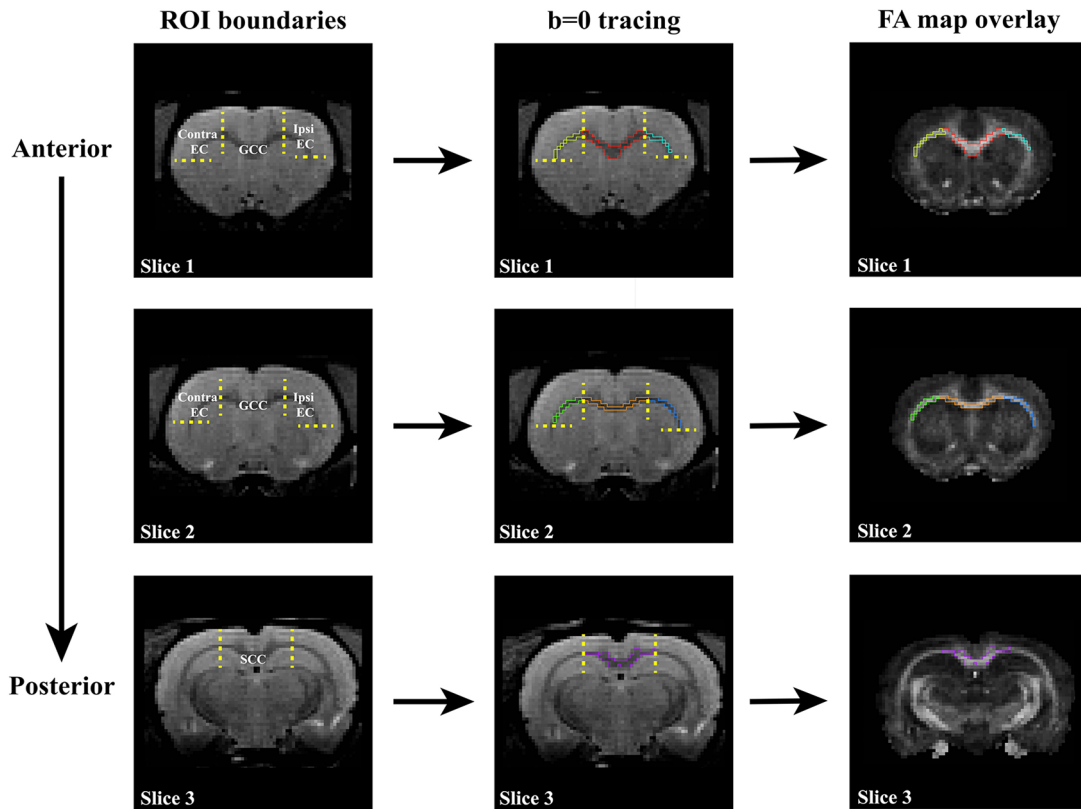


**Figure 3.** Manual tracing methods and ROI. Four ROIs were defined for each DTI acquisition: genu corpus callosum (GCC), splenium corpus callosum (SCC), ipsilateral external capsule (Ipsi EC), and contralateral external capsule (Contra EC), which were manually traced on 3 coronal slices of the  $b=0$  image. Following manual tracing, DTI parameters (FA, RD, MD, and AD) were extracted as the average across each ROI. AD indicates axial diffusivity, DTI, diffusion tensor imaging; FA, fractional anisotropy; MD, mean diffusivity; RD, radial diffusivity; ROI, region of interest.

skull fracture ( $n=1$ ) and intracerebral hemorrhage ( $n=1$ ). All animals were visually monitored following trauma for signs of abnormal wakefulness, gate, and feeding.

### MRI acquisition

Magnetic resonance imaging was conducted at least 3 days prior to injury to acquire baseline values (mTBI,  $n=19$ ; sham,  $n=9$ ), and subsequently at 4 follow-up time points after injury or sham injury: <4 hours (mTBI,  $n=24$ ; sham,  $n=7$ ), 48 hours (mTBI,  $n=20$ ; sham,  $n=6$ ), 1 week (mTBI,  $n=4$ ; sham,  $n=6$ ), and 2 weeks post-injury (mTBI,  $n=9$ ; sham,  $n=5$ ). Rats were anesthetized with isoflurane maintained at 1.5% throughout the duration of imaging while circulating warm air preserved a constant body temperature (38°C). Animals were placed in an MRI holder (M2M, Cleveland, OH) with ear-bar restraints, and a 12-mm receive-only surface coil (Doty Scientific, Columbia, SC) was placed on the head. All images were acquired with a 9.4T scanner (Agilent Technologies, Wilmington, DE) and a 90-mm birdcage-style transmit coil (M2M). Slices were placed consistently during acquisition with respect to the structures studied. Also, we used a custom head holder and great care in animal positioning to ensure consistent plane of section and slice position for each animal. Diffusion tensor imaging was achieved using a spin-echo (SE) approach

with fast-SE readout (echo factor 4) and 21 “electro-repulsive” diffusion directions including 1 with  $b=0\text{ s/cm}^2$  and 20 with  $b=800\text{ s/cm}^2$ , resolution =  $128 \times 128$ , 12-2 mm interleaved slices in an axial plane with 30 cm field of view, resulting in images of  $2.34 \times 2.34 \times 2\text{ mm}$  voxel size. High-resolution anatomical T1W and T2W images, acquired to insure the absence of gross abnormalities—that is, skull fractures, hemorrhaging, and edema—were reviewed after each session. The duration of each scan session was approximately 90 minutes. Diffusion tensor images were eddy current corrected and processed using the FMRIB Diffusion Toolbox<sup>24</sup> to estimate the diffusion tensor and to compute FA, MD, RD, and AD at each voxel.

### Tracing methods

One rater (W.S.H.), blind to group membership and MRI timing, manually traced the corpus callosum (genu and splenium) and bilateral external capsule on the  $b=0$  image of all DTI acquisitions ( $n=109$ ) using Medical Image Processing and Visualization software (MIPAV; version 8.0.2)<sup>25</sup> (Figure 3). These regions of interest (ROIs) were selected for their clinical relevance as they represent the most commonly reported locations of abnormal FA by ROI analyses in human DTI studies of TBI,<sup>26</sup> and they have the greatest volume of white matter and thus minimize partial volume effects.

The tracing method was adapted from a previously published study.<sup>17</sup> Briefly, a total of 4 ROIs per acquisition were carefully defined by anatomical boundaries on 3 different coronal slices (Figure 3): ROI 1—*genu corpus callosum (GCC)*—was traced on 2 contiguous slices starting with the anterior-most boundary being the first slice where the corpus callosum crosses at midline. The lateral boundaries of the genu were defined at the apex of the white matter near the cingulum; ROI 2—*splenium corpus callosum (SCC)*—was traced on the last slice where the corpus callosum crosses at midline. The lateral boundaries of the splenium were defined at the apex of the white matter near the cingulum; ROI 3—*ipsilateral external capsule (IEC)*—was traced in the left hemisphere on the same 2 slices as GCC starting at the lateral boundary of the GCC continuing to the apex of the most lateral white matter; ROI 4—*contralateral external capsule (CEC)*—was traced similar to ROI 3, but in the right hemisphere. Following manual tracing, DTI parameter values (FA, RD, MD, and AD) within each ROI were extracted as the mean across the entire ROI. Intra-rater and inter-rater reliability of our manual tracing method was assessed.

### Histological analyses

Our primary goal for histological analyses was to assess the severity of our injury paradigm, which was aimed at inducing mild injury in the absence of gross pathology. Gross abnormalities were determined by screening for skull fractures, hemorrhaging, and edema through the visual inspection of anatomical MR images, by visual inspection of the skull and brain after euthanasia and review of hematoxylin and eosin (H&E)-stained sections. At day 14, immediately following the final MRI, the brains were harvested for histological analyses. Animals were perfused with 4% paraformaldehyde in saline using a transcardiac approach. The brains were kept within the cranium and immersed in the perfusion medium for 48 hours before removal. Tissue sections were embedded in paraffin blocks and sections were stained with H&E for the evaluation of gross morphological injury in cortical gray matter regions, including areas underneath the impact site.

### Statistical methods

Stata was used for data analysis (StataCorp. 2013. Stata: Release 13. Statistical Software; StataCorp LP, College Station, TX), and GraphPad Prism was used for creating graphs (version 7.03 for Windows; GraphPad Software, La Jolla, CA; www.graphpad.com).

To assess the intra-rater and inter-rater reliability of our manual tracing method, we re-traced a random subset of 10 cases and calculated the intra-correlation coefficients (ICCs) for each ROI.

In primary analysis, a total of 109 serial MRI acquisitions were analyzed to examine the evolution of 4 DTI metrics (FA, RD, MD, and AD) in 4 different ROIs (GCC, SCC, IEC, and

CEC) following concussive or sham injury. Longitudinal trends (baseline, <4 hours post-injury, 48 hours post injury, 1 week post-injury, and 2 weeks post-injury) in DTI metrics for each group (sham, mTBI) were analyzed by linear mixed-effects (LME) models to account for repeated measures, missing longitudinal data points, and covariates. Under LME, a likelihood ratio test (LRT) on group  $\times$  time interaction was performed to assess the statistical significance for the difference of longitudinal trends between the sham and mTBI groups. More specifically, the LRT assessed the goodness of fit between 2 LME models: model 1—main effects (group + time) and model 2—main effects plus interaction (group + time + group  $\times$  time). A total of 16 LRTs were performed to assess the interaction for each DTI metric and ROI combination. To address the noise floor of DTI measurements and to reduce the probability of Type I error associated with multiple (16) LRT comparisons, we applied Bonferroni correction and set the level of statistical significance at  $P < .003$  ( $\alpha = 0.05/16$ ). Any interaction effects deemed significant were further described using descriptive statistics.

## Results

### Manual tracing and reliability analysis

Our manual tracing method yielded evenly sized ROIs across groups (GCC: mTBI =  $76 \pm 12$  voxels vs sham =  $74 \pm 13$  voxels,  $t = 0.59$ ,  $df = 107$ ,  $P = .56$ ; SCC: mTBI =  $50 \pm 9$  voxels vs sham =  $52 \pm 10$  voxels,  $t = 1.2$ ,  $df = 107$ ,  $P = .22$ ; IEC: mTBI =  $27 \pm 4$  voxels vs sham =  $28 \pm 4$  voxels,  $t = 1.5$ ,  $df = 107$ ,  $P = .15$ ; CEC: mTBI =  $27 \pm 4$  voxels vs sham =  $27 \pm 4$  voxels,  $t = 0.71$ ,  $df = 107$ ,  $P = .48$ ).

Furthermore, excellent intra-rater (W.S.H. vs W.S.H.) and inter-rater (W.S.H. vs J.L.) agreement was observed for all ROIs (ICC = 0.85–0.99, all  $P$ -values  $< .001$ ), which confirms that our manual tracing method can be reliably used for rat DTI data such as those collected in our study.

### DTI of the evolving response to mTBI

Longitudinal DTI metrics and LME results are presented in Table 1 and Figures 4 to 7. The LRT revealed significant interaction effects for FA of the GCC ( $\chi^2 = 19.92$ ,  $df = 4$ ,  $P = .0005$ ), RD of the GCC ( $\chi^2 = 18.64$ ,  $df = 4$ ,  $P = .0009$ ), and MD of the GCC ( $\chi^2 = 17.18$ ,  $df = 4$ ,  $P = .002$ ). All other LRTs did not reach statistical significance after Bonferroni correction. There were no statistically significant differences at baseline in DTI measurements between sham and mTBI animals.

*FA of the GCC following mTBI.* Overall, the evolution of FA in the GCC following concussive or sham injury differed by group ( $\chi^2 = 19.92$ ,  $df = 4$ ,  $P = .0005$ ; Figure 4E). In contrast to the sham group, mTBI animals initially showed a mild decrease in FA ( $-5.7\%$ ) from baseline to immediately after injury (baseline FA = 0.678, 95% confidence interval [CI] = 0.647–0.710 vs

**Table 1.** DTI values and linear mixed-effects analysis.

DTI METRIC ↓	ROI ↓	mTBI	SHAM							STATISTICS						
			BASELINE		48 HOURS	1 WEEK	2 WEEKS	BASELINE	<4 HOURS	48 HOURS	1 WEEK	2 WEEKS	LME MODEL 1 <sup>a</sup>	LME MODEL 2 <sup>b</sup>	LIKELIHOOD RATIO TEST	P-VALUE
			LOGLIK	LOGLIK	LOGLIK	LOGLIK	LOGLIK	LOGLIK	LOGLIK	LOGLIK	LOGLIK	LOGLIK	LOGLIK	LOGLIK	CHI SQUARE	P-VALUE
FA	GCC	0.678	0.640	0.666	0.799	0.659	0.608	0.690	0.658	0.661	0.689	136.2	146.1	19.92	0.0005*	
		(0.065)	(0.073)	(0.086)	(0.027)	(0.048)	(0.087)	(0.072)	(0.027)	(0.040)	(0.087)					
		0.660	0.658	0.698	0.767	0.689	0.671	0.744	0.693	0.669	0.691	140.7	148.0	14.53	0.006	
		(0.079)	(0.066)	(0.070)	(0.052)	(0.057)	(0.057)	(0.060)	(0.023)	(0.056)	(0.087)					
IEC	GCC	0.563	0.541	0.579	0.675	0.582	0.517	0.557	0.534	0.536	0.625	134.0	140.9	13.75	0.008	
		(0.059)	(0.075)	(0.070)	(0.043)	(0.067)	(0.081)	(0.107)	(0.036)	(0.061)	(0.056)					
		0.576	0.535	0.593	0.655	0.564	0.492	0.553	0.585	0.575	0.610	138.0	145.4	14.90	0.005	
		(0.074)	(0.056)	(0.085)	(0.031)	(0.053)	(0.085)	(0.031)	(0.048)	(0.083)						
RD	GCC	0.274	0.318	0.295	0.167	0.299	0.340	0.263	0.258	0.283	0.258	885.2	894.5	18.64	0.0009*	
		(0.066)	(0.077)	(0.085)	(0.041)	(0.085)	(0.076)	(0.067)	(0.032)	(0.049)	(0.085)					
		0.317	0.313	0.281	0.208	0.289	0.308	0.247	0.263	0.298	0.270	891.8	895.8	8.04	0.090	
		(0.093)	(0.069)	(0.060)	(0.038)	(0.083)	(0.057)	(0.059)	(0.032)	(0.050)						
IEC	GCC	0.309	0.331	0.297	0.213	0.289	0.351	0.306	0.309	0.320	0.253	885.0	890.0	10.08	0.039	
		(0.070)	(0.075)	(0.077)	(0.032)	(0.093)	(0.093)	(0.073)	(0.050)	(0.046)	(0.052)					
		0.302	0.340	0.299	0.225	0.316	0.358	0.317	0.264	0.299	0.272	892.8	898.4	11.27	0.024	
		(0.068)	(0.065)	(0.082)	(0.031)	(0.078)	(0.070)	(0.056)	(0.299)	(0.061)						
MD	GCC	0.512	0.558	0.531	0.429	0.540	0.563	0.505	0.460	0.512	0.487	887.6	896.2	17.18	0.002*	
		(0.070)	(0.073)	(0.076)	(0.055)	(0.109)	(0.050)	(0.060)	(0.052)	(0.056)	(0.070)					
		0.573	0.559	0.537	0.480	0.554	0.550	0.529	0.500	0.555	0.519	887.7	889.8	4.15	0.386	
		(0.096)	(0.075)	(0.057)	(0.042)	(0.103)	(0.045)	(0.047)	(0.034)	(0.058)						
IEC	GCC	0.468	0.487	0.449	0.372	0.442	0.511	0.459	0.451	0.469	0.411	888.1	893.4	10.64	0.031	
		(0.077)	(0.075)	(0.071)	(0.048)	(0.048)	(0.077)	(0.053)	(0.062)	(0.047)	(0.052)					
		0.466	0.498	0.461	0.389	0.477	0.506	0.473	0.404	0.456	0.429	889.0	893.8	9.59	0.048	
		(0.072)	(0.070)	(0.081)	(0.040)	(0.096)	(0.051)	(0.061)	(0.072)	(0.067)						
AD	GCC	0.987	1.038	1.004	0.953	1.021	1.010	0.988	0.865	0.969	0.945	854.5	859.7	10.33	0.035	
		(0.098)	(0.094)	(0.103)	(0.093)	(0.167)	(0.075)	(0.089)	(0.108)	(0.071)	(0.045)					
		1.084	1.051	1.051	1.025	1.084	1.033	1.093	0.975	1.069	1.017	832.1	834.2	4.19	0.381	
		(0.130)	(0.129)	(0.112)	(0.130)	(0.160)	(0.086)	(0.056)	(0.125)	(0.119)						
IEC	GCC	0.786	0.800	0.754	0.690	0.749	0.833	0.763	0.733	0.766	0.727	869.9	874.3	8.72	0.069	
		(0.100)	(0.094)	(0.091)	(0.089)	(0.108)	(0.087)	(0.036)	(0.092)	(0.064)	(0.059)					
		0.793	0.814	0.784	0.717	0.799	0.802	0.786	0.684	0.770	0.741	863.8	866.8	6.02	0.198	
		(0.089)	(0.090)	(0.101)	(0.060)	(0.141)	(0.053)	(0.088)	(0.096)	(0.054)						

Abbreviations: AD, axial diffusivity; CEC, contralateral external capsule; DTI, diffusion tensor imaging; FA, fractional anisotropy; GCC, genu corpus callosum; IEC, ipsilateral external capsule; LME, linear mixed-effects; LogLik, log likelihood; MD, mean diffusivity; RD, radial diffusivity; ROI, region of interest; SCC, splenium corpus callosum.  
 DTI values are reported as mean (SD); the RD, MD, and AD values are x1000 (mm<sup>2</sup>/s).  
<sup>a</sup>Group (mTBI, sham) + time (baseline, <4 hours, 48 hours, 1 week, 2 weeks).  
<sup>b</sup>Group (mTBI, sham) + time (baseline, <4 hours, 48 hours, 1 week, 2 weeks) + group × time.  
 \*Significant after Bonferroni correction,  $P < .003$  ( $\alpha = 0.05/16$ ).

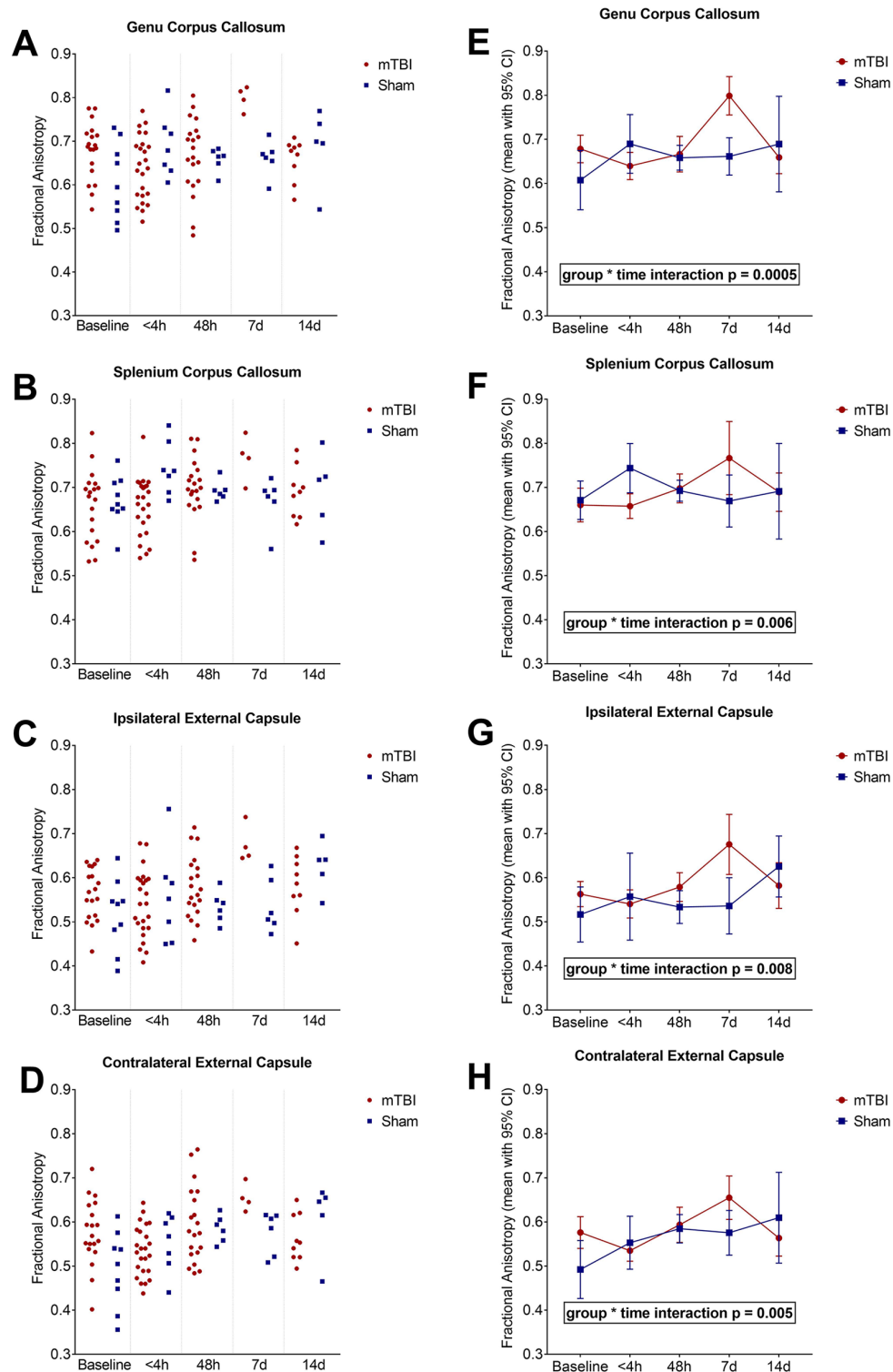


**Figure 4.** Scatterplots (A-D) and trend lines (E-H) for the evolution of fractional anisotropy (FA) following concussive or sham injury in various ROIs. Each dot in the scatterplots represents a single animal. Trend lines are depicted as mean with 95% confidence interval. mTBI indicates mild traumatic brain injury; ROI, region of interest.

<4-hour FA=0.640, 95% CI=0.609-0.671). Then, FA rebounded and mildly increased (+4.2%) 48 hours post-injury (48-hour FA=0.666, 95% CI=0.626-0.707). However, the most dramatic change in FA was observed at 1 week post-injury—that is, FA was increased by +17.8% vs baseline, +24.9% vs <4 hours, +19.8% vs 48 hours, and +20.8% vs sham at 1 week. Finally, FA returned to baseline values 2 weeks

after concussive injury (2-week FA=0.659, 95% CI=0.622-0.696).

*RD of the GCC following mTBI.* Overall, the evolution of RD in the GCC following concussive or sham injury differed by group ( $\chi^2=18.64$ ,  $df=4$ ,  $P=.0009$ ; Figure 5E). Whereas the RD values initially decreased in sham animals, they increased by +16.3% in

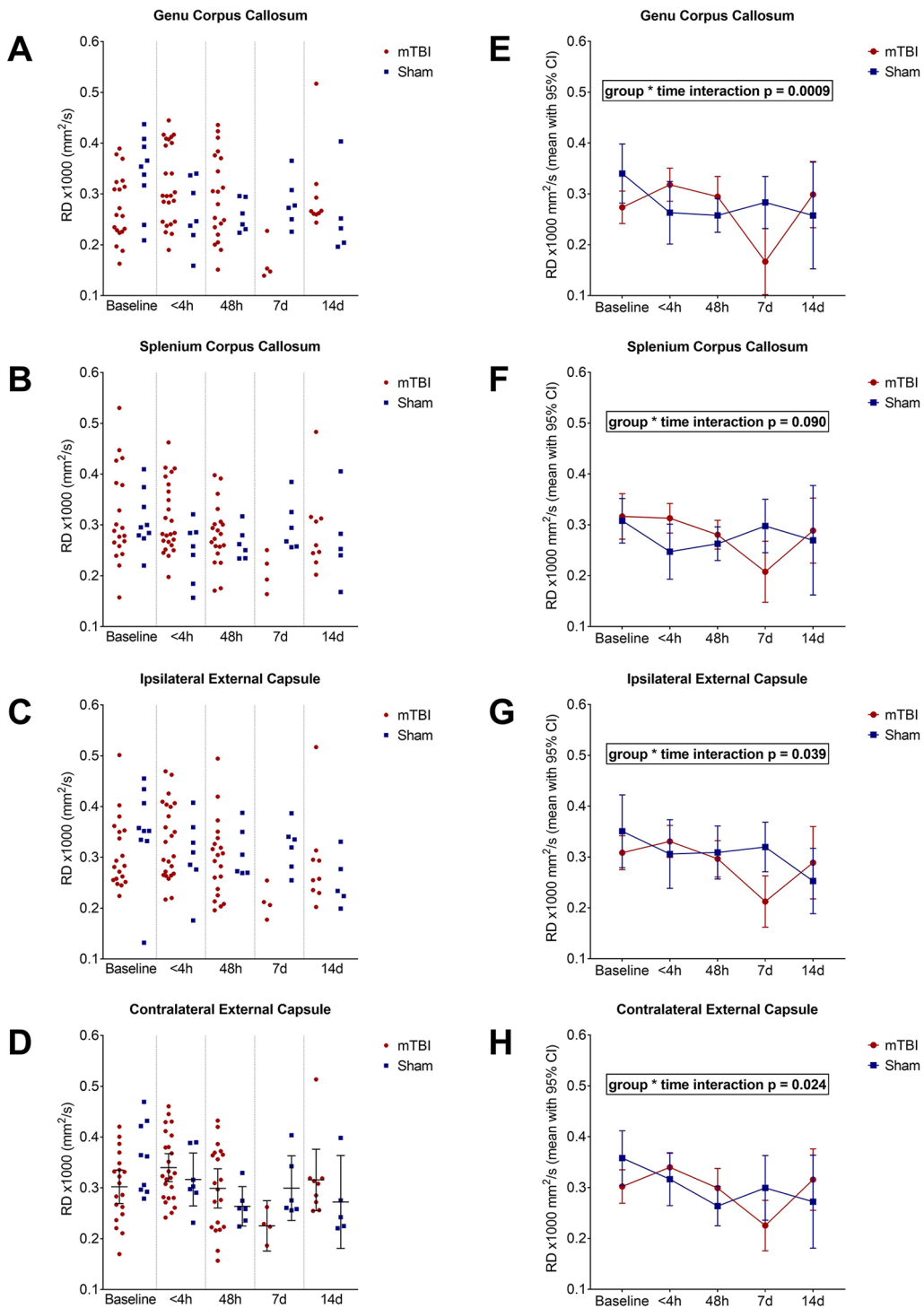


**Figure 5.** Scatterplots (A-D) and trend lines (E-H) for the evolution of radial diffusivity (RD) following concussive or sham injury in various ROIs. Each dot in the scatterplots represents a single animal. Trend lines are depicted as mean with 95% confidence interval. mTBI indicates mild traumatic brain injury; ROI, region of interest.

mTBI animals (baseline RD=0.274, 95% CI=0.242-0.306 vs <4-hour RD=0.318, 95% CI=0.286-0.351). At 48 hours post-injury (48-hour RD=0.295, 95% CI=0.255-0.334), RD started to rebound (-7.4% vs <4 hours) and continued to maximum decreased RD values at 1 week post-injury (1-week RD=0.167, 95% CI=0.102-0.232). Specifically, at 1 week post-injury, the RD values were decreased by -39.0% vs baseline, -47.5% vs

4 hours, -43.3% vs 48 hours, and -41.1% vs sham animals at 1 week. Finally, RD returned to baseline values 2 weeks after concussive injury (2-week RD=0.299, 95% CI=0.234-0.364).

*MD of the GCC following mTBI.* Overall, the evolution of MD in the GCC following concussive or sham injury differed by group ( $\chi^2 = 17.18, df = 4, P = .002$ ; Figure 6E). In contrast to the

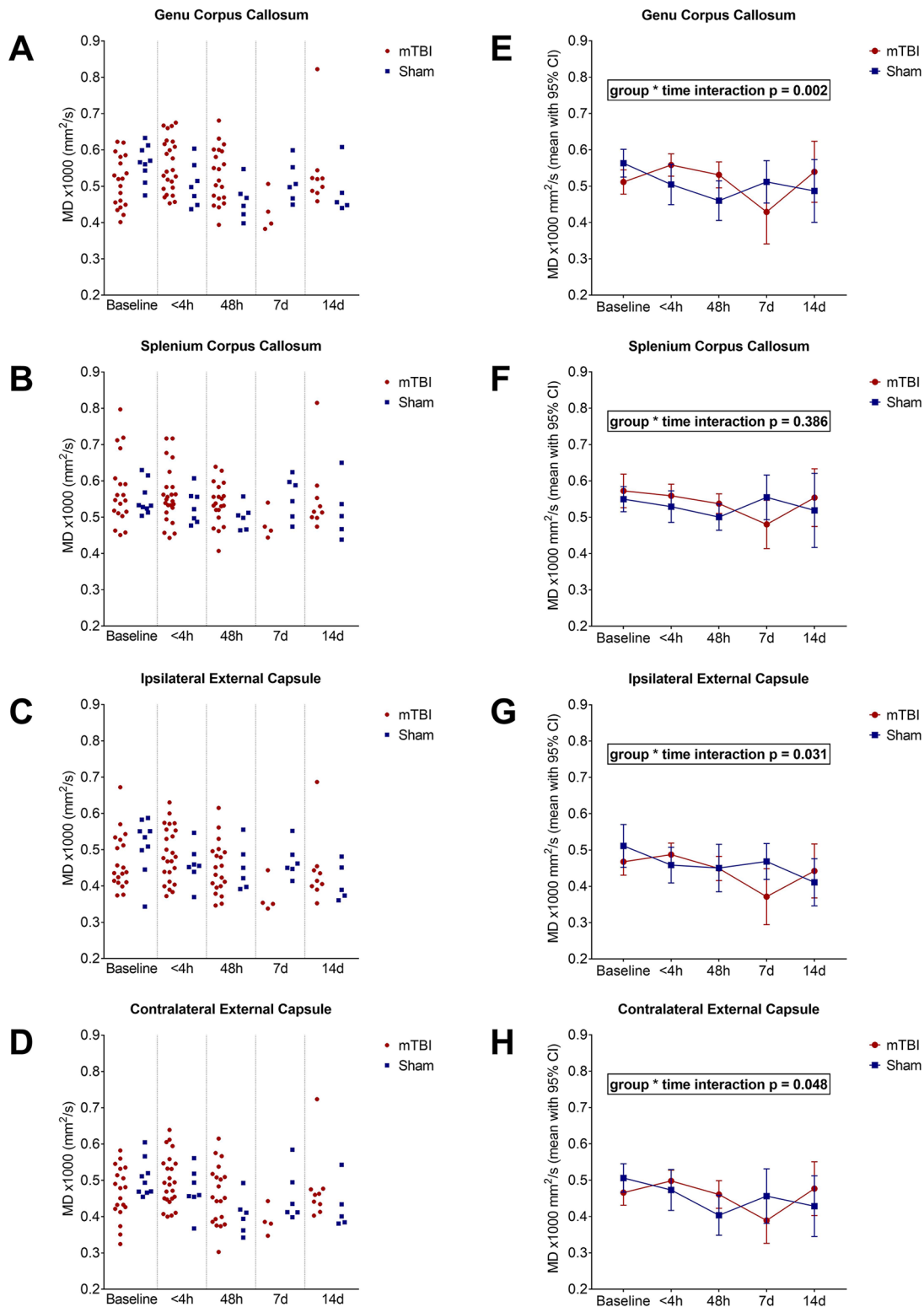


**Figure 6.** Scatterplots (A-D) and trend lines (E-H) for the evolution of mean diffusivity (MD) following concussive or sham injury in various ROIs. Each dot in the scatterplots represents a single animal. Trend lines are depicted as mean with 95% confidence interval. mTBI indicates mild traumatic brain injury; ROI, region of interest.

sham group, mTBI animals showed a mild increase (+9.1%) in MD at <4 hours post-injury vs baseline (baseline MD=0.512, 95% CI=0.478-0.545 vs <4-hour MD=0.558, 95% CI=0.527-0.589). At 48 hours post-injury (48-hour MD=0.531, 95% CI=0.496-0.567), MD started to rebound

(-4.8% vs <4 hours) and continued to maximum decreased MD values at 1 week post-injury (1-week MD=0.429, 95% CI=0.341-0.517). Specifically, at 1 week post-injury, the MD values were decreased by -39.0% vs baseline, -47.5% vs 4 hours, -43.3% vs 48 hours, and -41.1% vs sham animals at 1 week.



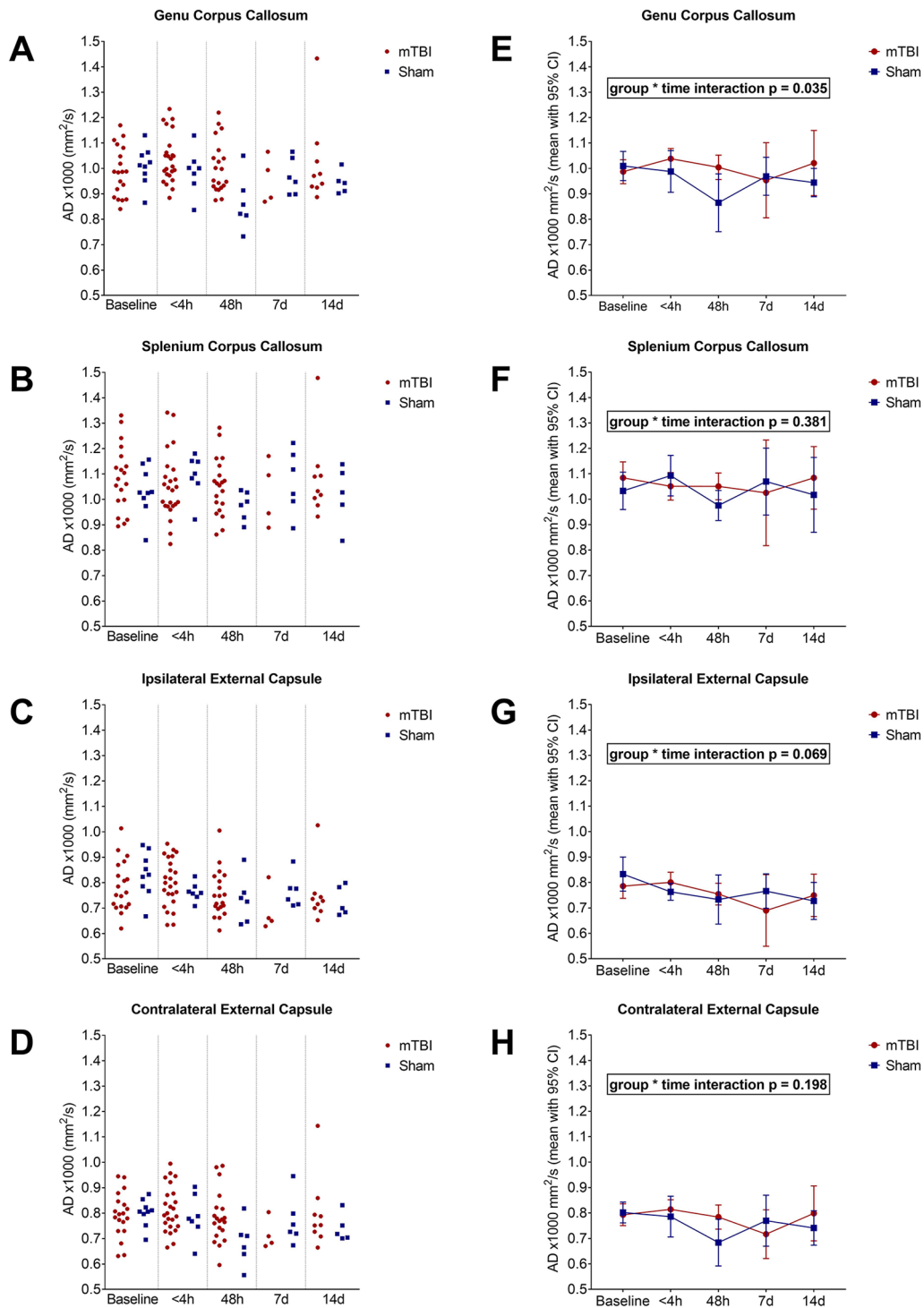


**Figure 7.** Scatterplots (A-D) and trend lines (E-H) for the evolution of axial diffusivity (AD) following concussive or sham injury in various ROIs. Each dot in the scatterplots represents a single animal. Trend lines are depicted as mean with 95% confidence interval. mTBI indicates mild traumatic brain injury; ROI, region of interest.

Finally, MD returned to baseline values 2 weeks after concussive injury (2-week MD = 0.659, 95% CI = 0.622-0.696).

#### Pathological examination

Rats sacrificed at 2 weeks post-injury did not reveal any gross abnormalities as indicated by the visual inspection of

anatomical MR images, by visual inspection of the skull and brain after euthanasia (ie, no skull fractures, hemorrhaging, and edema) and review of H&E-stained brain sections.

#### Discussion

In this study, we used a rodent model of mTBI to investigate longitudinal indices of axonal injury. A single, very mild,

closed-skull head impact resulted in detectable changes by DTI in rats in the absence of gross abnormalities as indicated by visual screening of anatomical MRI and by review of H&E-stained brain sections. Diffusion tensor imaging changes within the white matter were not immediately apparent, but developed at 1 week post-injury and returned to baseline values by 2 weeks post-injury. These findings underscore the evolving nature of brain injury after concussion.

Fractional anisotropy, which assesses the coherence of water diffusion, has been used to assess overall white matter integrity in both animal and human studies of traumatic brain injury (TBI).<sup>16,18,19,26</sup> In our model, the evolution of FA in the GCC following concussive or sham injury differed by group and yielded a noticeable FA increase at 1 week post-injury. Increased FA in the early injury phase following mTBI has also been reported by other animal studies. For example, Kikinis and colleagues<sup>27</sup> investigated *ex vivo* DTI 1 week after single mTBI was induced by impact to the left parietal bone in adult male Sprague Dawley rats. They found increased FA compared with shams mainly in contrecoup regions, including the pyramidal tract, cerebral peduncle, superior cerebellar peduncle, corpus callosum, anterior commissure, the fimbria of the hippocampus, fornix, medial forebrain, and optic chiasm. Furthermore, Herrera and colleagues<sup>19</sup> used a single concussive impact model without skull fracture to assess pathophysiological changes at 72 hours post-injury in adult male Sprague Dawley rats and found significantly increased FA in the internal capsule compared with pre-injury baseline. Qin and colleagues<sup>16</sup> found increased FA at 1 week post-injury in rats that returned to pre-injury values after 2 to 3 weeks, although this finding was limited to gray matter regions (ie, cortex and hippocampus) and only after repetitive, not single mTBI. Conversely, reduced FA has also been reported. For example, Haber and colleagues<sup>28</sup> performed *ex vivo* MRI in mice 1 week following 2 head impacts (spaced 24 hours apart) using the Closed Head Injury Model of Engineered Rotational Acceleration (CHIMERA). They reported reduced FA compared with sham in various brain regions, including the hippocampus. Interestingly, their findings were also correlated with histological markers of axonal damage and gliosis. Many differences in experimental conditions and design may explain the divergence of findings from those we report. These include differences such as the adopted injury model (direct head impact vs CHIMERA), injury paradigm (single vs repeated impacts), species used (rats vs mice), MRI acquisition (*in vivo* vs *ex vivo*), sample size, scanner gradient performance, partial volume effects, and methods for data post-processing. In fact, a current major challenge in rodent TBI studies is the experimental variability and reproducibility of findings among different labs.<sup>29,30</sup> Notably, TBI manifestations are highly heterogeneous among humans suggesting that concussion is not a uniform disease. For this reason, various animal models may be needed to encompass the spectrum of TBI.

The review and meta-analysis by Eierud and colleagues<sup>31</sup> support the hypothesis that elevated anisotropy is an acute phenomenon and depressed anisotropy is the result of chronic injury. However, in another review,<sup>26</sup> low FA was reported in most TBI articles examined regardless of the time of injury and across various injury severities. Although we did not assess chronic FA changes as our animals were only studied for 2 weeks, our 1-week increased FA findings are in line with human concussion studies reporting increased FA in acute brain injury.<sup>22,32-36</sup> For example, Mayer and colleagues<sup>32</sup> found that patients with semi-acute mTBI (12 days post-injury) had greater FA due to lower RD in the corpus callosum and several left hemisphere tracts compared with healthy controls. Moreover, longitudinal data (3-5 months post-injury) provided evidence of partial normalization of DTI values in mTBI patients. In another study, Yallampalli and colleagues<sup>33</sup> found that, compared with controls, mTBI patients who suffered concussion 1 to 6 days prior to DTI acquisition had elevated fornix FA.

Results from FA alone, however, are insufficient to confirm specific pathologic mechanisms. Evaluation of additional DTI parameters may permit meaningful inferences regarding pathomechanisms. In the context of subacute mild TBI, high FA in combination with low RD is hypothesized to reflect inflammation or axonal cytotoxic edema.<sup>16,22,32,34,37</sup> For example, Wilde and colleagues<sup>22</sup> performed DTI 1 to 6 days post-injury in adolescents with mTBI and found higher FA in combination with lower RD and AD values for the whole corpus callosum compared with controls. These DTI values were also correlated with the severity of post-concussive symptoms in the mTBI group, but not in the control group. Similarly, Bazarian and colleagues<sup>34</sup> reported elevated FA and decreased trace in the anterior limb of the internal capsule and in the posterior portion of the corpus callosum assessed at 72 hours post-injury in mTBI patients vs healthy controls. These findings were deemed suggestive of axonal swelling, an early step in the process of axonal injury.

In line with these reports, we detected a coincident increase of FA post-injury with a decline of RD and MD in the corpus callosum at 1 week, but no significant change in AD. Neuropathology following concussion is believed to be the result of rapid deformation of the brain tissue.<sup>38</sup> Rapid acceleration and deceleration of the brain results in stretching of axons, which are thought to alter the function of gated ion channels causing an influx of water into cells, which is associated with a decrease in extracellular water, a process known as cytotoxic edema.<sup>32,39</sup> The pattern of change in DTI parameters in our model may correspond to localized inflammatory responses or cytotoxic edema as a mechanism of injury although additional histopathological characterization is required to better understand the neurobiological correlates of our DTI measures. Given that the signal detected by DTI arises from the extracellular space, directionally restricted diffusion (high FA,

low RD, and low MD) is consistent with compression of the extracellular space possibly due to axonal swelling. The absence of changes in AD suggests the absence of axonal loss. Resolution of diffusion changes by 2 weeks post-injury is further supportive of the evolution and subsequent resolution of edema without axonal loss. It should be noted, however, that great care must be used when interpreting DTI changes as DTI is not specific to a particular pathological mechanism. It is unclear, for example, whether changes in FA are the result of abnormalities of myelin, axolemma, inflammation, or other factors.<sup>5</sup> Therefore, our findings should be considered preliminary and require further histopathologic characterization.

Furthermore, the time course of our findings is consistent with a similar model of closed-skull mild TBI in mice.<sup>17</sup> Bennett and colleagues did not observe acute DTI changes (24 hours) within white matter (ie, corpus callosum and external capsule), but a significant reduction of MD was observed only after 7 days post-injury compared with sham-injured animals and to acute-phase DTI. However, Bennett and colleagues also observed significantly reduced AD at 7 days (in the absence of amyloid precursor protein (APP) pathology), which was attributed to axonal degeneration and diverges from our findings (of unchanged AD over time). It is plausible that the divergence of AD effects from our study arises from more severe injury (2 impacts 24 hours apart at 3.3 mm impact depth used by Bennett and colleagues vs 1 impact at 2 mm impact depth used in our model).

Of note, some of the DTI changes we observed in sham animals may be attributed to the neuromodulatory effects of (repeated) general anesthesia.<sup>40,41</sup> This idea is supported by the fact that most of the DTI changes in sham animals were observed between baseline and 48 hours post-sham injury, which was the most anesthesia-intense timeframe in our study (3 episodes of general anesthesia in 5 days). Our study was not designed to specifically disentangle anesthetic effects, which is an important area for future study.

Our findings must be considered in the context of several limitations. First, our sample size for the 1-week follow-up was relatively small (ie,  $n = 4$  for mTBI vs  $n = 6$  for sham) and, therefore, related findings should be considered preliminary. However, the scatterplots in Figures 4 to 7 confirm a highly homogeneous distribution of measurements—that is, outliers do not drive the findings and the “1-week effect” was not evident in sham-injured animals.

Second, H&E staining alone is inadequate to evaluate mTBI pathology. Additional histopathologic assessment—including evaluation of myelin, inflammation, and axonal injury—is needed for a more complete characterization of the injury response and a better understanding of how DTI metrics are correlated with cellular responses. Unfortunately, these measures were beyond the scope of our current MRI study and represent an important study limitation. Despite the lack of additional histopathologic evaluation, we believe that our study is of broad interest and motivates future study including more

detailed histopathology as there are few or no imaging markers to predict the mTBI outcome.

Third, our follow-up was limited to 2 weeks. Although most DTI changes returned to baseline values after 2 weeks, we cannot exclude the possibility of ongoing microstructural white matter changes beyond 2 weeks. In a recent ferret model of mTBI, FA reductions in the white matter regions not proximate to the site of impact were most pronounced at later time points (ie, 4–16 weeks).<sup>21</sup>

Fourth, even though we selected the largest white matter areas and consistently traced ROIs, partial volume effects may have influenced our DTI results and decreased the statistical power of our DTI analysis. Despite the partial volume limitation, we were able to detect significant DTI changes, which is a motivator to pursue further higher resolution imaging that may thus reveal more. To minimize partial volume effects, future studies should consider a high image resolution with isotropic voxels.<sup>42</sup>

Finally, our study was limited to a single mild head impact and cannot address the role of multiple and repetitive impacts that reflect important TBI contexts such as sports- and military-related concussions and the potential cumulative effects of repetitive head impacts.


In conclusion, we employed a longitudinal design to study the response of the brain at multiple time points over a 2-week period following concussive injury in an animal model of mTBI. In our study, microstructural white matter changes evolved differently between groups following concussive or sham injury with noticeable DTI changes at 1 week post-injury. Whereas additional histopathologic characterization is required to better understand the neurobiological correlates of DTI measures, our findings highlight the evolving nature of the brain's response to injury following concussion.

### Author Contributions

CAB and MLL conceived and led the project. CAB, MHC, and KB performed experiments. CAB, MHC and WSH processed imaging data. WSH and JL traced regions-of-interest. WSH and KY analyzed the data. WSH wrote the main manuscript text and created all tables, figures, art work and photos. All authors reviewed, edited and approved the final version of the manuscript.

### ORCID iDs

Todd G Rubin  <https://orcid.org/0000-0002-2821-5877>

Michael L Lipton  <https://orcid.org/0000-0002-4702-2114>

### REFERENCES

1. Gardner RC, Yaffe K. Epidemiology of mild traumatic brain injury and neurodegenerative disease. *Mol Cell Neurosci*. 2015;66:75–80.
2. Rosenbaum SB, Lipton ML. Embracing chaos: the scope and importance of clinical and pathological heterogeneity in mTBI. *Brain Imaging Behav*. 2012;6:255–282.
3. Lo C, Shifteh K, Gold T, Bello JA, Lipton ML. Diffusion tensor imaging abnormalities in patients with mild traumatic brain injury and neurocognitive impairment. *J Comput Assist Tomogr*. 2009;33:293–297.

4. Mayer AR, Quinn DK, Master CL. The spectrum of mild traumatic brain injury: a review. *Neurology*. 2017;89:623–632.
5. Shenton ME, Hamoda HM, Schneiderman JS, et al. A review of magnetic resonance imaging and diffusion tensor imaging findings in mild traumatic brain injury. *Brain Imaging Behav*. 2012;6:137–192.
6. Basser PJ, Mattiello J, LeBihan D. MR diffusion tensor spectroscopy and imaging. *Biophys J*. 1994;66:259–267.
7. Basser PJ, Pierpaoli C. Microstructural and physiological features of tissues elucidated by quantitative-diffusion-tensor MRI. *J Magn Reson B*. 1996;111:209–219.
8. Budde MD, Kim JH, Liang HF, et al. Toward accurate diagnosis of white matter pathology using diffusion tensor imaging. *Magn Reson Med*. 2007;57:688–695.
9. Lipton ML, Kim N, Park YK, et al. Robust detection of traumatic axonal injury in individual mild traumatic brain injury patients: intersubject variation, change over time and bidirectional changes in anisotropy. *Brain Imaging Behav*. 2012;6:329–342.
10. O'Connor WT, Smyth A, Gilchrist MD. Animal models of traumatic brain injury: a critical evaluation. *Pharmacol Ther*. 2011;130:106–113.
11. Xiong Y, Mahmood A, Chopp M. Animal models of traumatic brain injury. *Nat Rev Neurosci*. 2013;14:128–142.
12. Shultz SR, McDonald SJ, Vonder Haar C, et al. The potential for animal models to provide insight into mild traumatic brain injury: translational challenges and strategies. *Neurosci Biobehav Rev*. 2017;76:396–414.
13. Bolouri H, Zetterberg H. Animal models for concussion: molecular and cognitive assessments—relevance to sport and military concussions. In: Kobeissy FH ed. *Brain Neurotrauma: Molecular, Neuropsychological, and Rehabilitation Aspects*. Boca Raton, FL: CRC Press; 2015. <https://www.ncbi.nlm.nih.gov/pubmed/26269898>.
14. Ma X, Aravind A, Pfister BJ, Chandra N, Haorah J. Animal models of traumatic brain injury and assessment of injury severity [published online ahead of print January 2, 2019]. *Mol Neurobiol*. doi:10.1007/s12035-018-1454-5.
15. Mac Donald CL, Dikranian K, Bayly P, Holtzman D, Brody D. Diffusion tensor imaging reliably detects experimental traumatic axonal injury and indicates approximate time of injury. *J Neurosci*. 2007;27:11869–11876.
16. Qin Y, Li GL, Xu XH, Sun ZY, Gu JW, Gao FB. Brain structure alterations and cognitive impairment following repetitive mild head impact: an in vivo MRI and behavioral study in rat. *Behav Brain Res*. 2016;340:41–48.
17. Bennett RE, Mac Donald CL, Brody DL. Diffusion tensor imaging detects axonal injury in a mouse model of repetitive closed-skull traumatic brain injury. *Neurosci Lett*. 2012;513:160–165.
18. Mannix R, Meehan WP, Mandeville J, et al. Clinical correlates in an experimental model of repetitive mild brain injury. *Ann Neurol*. 2013;74:65–75.
19. Herrera JJ, Bockhorst K, Kondraganti S, Stertz L, Quevedo J, Narayana PA. Acute white matter tract damage after frontal mild traumatic brain injury. *J Neurotrauma*. 2017;34:291–299.
20. Mac Donald CL, Dikranian K, Song SK, Bayly PV, Holtzman DM, Brody DL. Detection of traumatic axonal injury with diffusion tensor imaging in a mouse model of traumatic brain injury. *Exp Neurol*. 2007;205:116–131.
21. Hutchinson EB, Schwerin SC, Radomski KL, et al. Detection and distinction of mild brain injury effects in a ferret model using diffusion tensor MRI (DTI) and DTI-driven tensor-based morphometry (D-TBM). *Front Neurosci*. 2018;12:573.
22. Wilde EA, McCauley SR, Hunter JV, et al. Diffusion tensor imaging of acute mild traumatic brain injury in adolescents. *Neurology*. 2008;70:948–955.
23. National Research Council (US) Committee for the Update of the Guide for the Care and Use of Laboratory Animals, Institute for Laboratory Animal Research (US). *Guide for the Care and Use of Laboratory Animals*. 8th ed. Washington, DC: National Academies Press; 2011 [http://www.nap.edu/catalog.php?record\\_id=12910](http://www.nap.edu/catalog.php?record_id=12910).
24. Smith SM, Johansen-Berg H, Jenkinson M, et al. Acquisition and voxelwise analysis of multi-subject diffusion data with tract-based spatial statistics. *Nat Protoc*. 2007;2:499–503.
25. McAuliffe MJ, Lalonde FM, McGarry D, Gandler W, Csaky KBLT. Medical image processing, analysis & visualization in clinical research. Paper presented at: IEEE Computer-Based Medical Systems (CBMS); July 26–27, 2001; Bethesda, MD.
26. Hulkower MB, Poliak DB, Rosenbaum SB, Zimmerman ME, Lipton ML. A decade of DTI in traumatic brain injury: 10 years and 100 articles later. *AJNR*. 2013;34:2064–2074.
27. Kikinis Z, Muehlmann M, Pasternak O, et al. Diffusion imaging of mild traumatic brain injury in the impact accelerated rodent model: a pilot study. *Brain Inj*. 2017;31:1376–1381.
28. Haber M, Hutchinson EB, Sadeghi N, et al. Defining an analytic framework to evaluate quantitative MRI markers of traumatic axonal injury: preliminary results in a mouse closed head injury model [published online ahead of print September 13, 2017]. *eNeuro*. doi:10.1523/ENEURO.0164-17.2017.
29. Namjoshi DR, Good C, Cheng WH, et al. Towards clinical management of traumatic brain injury: a review of models and mechanisms from a biomechanical perspective. *Dis Model Mech*. 2013;6:1325–1338.
30. Hoogenboom WS, Branch CA, Lipton ML. Animal models of closed-skull, repetitive mild traumatic brain injury. *Pharmacol Ther*. 2019;198:109–122.
31. Eierud C, Craddock RC, Fletcher S, et al. Neuroimaging after mild traumatic brain injury: review and meta-analysis. *Neuroimage Clin*. 2014;4:283–294.
32. Mayer AR, Ling J, Mannell MV, et al. A prospective diffusion tensor imaging study in mild traumatic brain injury. *Neurology*. 2010;74:643–650.
33. Yallampalli R, Wilde EA, Bigler ED, et al. Acute white matter differences in the fornix following mild traumatic brain injury using diffusion tensor imaging. *J Neuroimaging*. 2013;23:224–227.
34. Bazarian JJ, Zhong J, Blyth B, Zhu T, Kavcic V, Peterson D. Diffusion tensor imaging detects clinically important axonal damage after mild traumatic brain injury: a pilot study. *J Neurotrauma*. 2007;24:1447–1459.
35. Pasternak O, Koerte IK, Bouix S, et al. Hockey concussion education project, part 2. *J Neurosurg*. 2014;120:873–881.
36. Henry LC, Tremblay J, Tremblay S, et al. Acute and chronic changes in diffusivity measures after sports concussion. *J Neurotrauma*. 2011;28:2049–2059.
37. Ling JM, Pena A, Yeo RA, et al. Biomarkers of increased diffusion anisotropy in semi-acute mild traumatic brain injury: a longitudinal perspective. *Brain*. 2012;135:1281–1292.
38. Cullen DK, Harris JP, Browne KD, et al. A porcine model of traumatic brain injury via head rotational acceleration. *Methods Mol Biol*. 2016;1462:289–324.
39. Rosenblum WI. Cytotoxic edema: monitoring its magnitude and contribution to brain swelling. *J Neuropathol Exp Neurol*. 2007;66:771–778.
40. Jevtovic-Todorovic V, Olney JW. PRO: anesthesia-induced developmental neuroapoptosis: status of the evidence. *Anesth Analg*. 2008;106:1659–1663.
41. Vutskits L, Xie Z. Lasting impact of general anaesthesia on the brain: mechanisms and relevance. *Nat Rev Neurosci*. 2016;17:705–717.
42. Kubicki M, McCarley R, Westin CF, et al. A review of diffusion tensor imaging studies in schizophrenia. *J Psychiatr Res*. 2007;41:15–30.